Original Article

Images of giant cell tumor and chondroblastoma around the knee: retrospective analysis of 99 cases

Jie-Lin Ma[1#], Yuan Wu[2#], Jin-Xu Wen[3], Zhi-Wei Zhong[3], Bao-Hai Yu[3], Chang Liu[3], Lei Cao[3], Tao Sun[4], Shu-Man Han[3], Bu-Lang Gao[5], Wen-Juan Wu[3]

[1]Department of Oncology, The Third Hospital of Hebei Medical University, Shijiazhuang, China; [2]Hebei Provincial Gucheng Hospital, Hengshui, China; [3]Department of Radiology, The Third Hospital of Hebei Medical University, Shijiazhuang, China; [4]Department of Bone and Soft Tissue Tumors, The Third Hospital of Hebei Medical University, Shijiazhuang, China; [5]Department of Medical Research, Shijiazhuang People's Hospital, Shijiazhuang, China

Contributions: (I) Conception and design: JL Ma, BH Yu, WJ Wu; (II) Administrative support: WJ Wu; (III) Provision of study materials or patients: JL Ma, BH Yu, Y Wu, C Liu; (IV) Collection and assembly of data: JL Ma, BH Yu, Y Wu, C Liu; (V) Data analysis and interpretation: BH Yu, WJ Wu, BL Gao; (VI) Manuscript writing: All authors; (VII) Final approval of manuscript: All authors.

[#]These authors contributed equally to this work.

Correspondence to: Zhi-Wei Zhong; Bao-Hai Yu. Department of Radiology, The Third Hospital of Hebei Medical University, 139 Ziqiang Road, Shijiazhuang 050051, China. Email: zhongzhiw@sina.com; yubaohai2002@163.com.

Background: It is difficult to differentiate giant cell tumors of the bone (GCTB) from chondroblastoma around the knee based on imaging findings. This study analyzed the imaging features of these 2 diseases for better differentiation.

Methods: This retrospective cross-sectional cohort study reviewed data of patients with pathologically confirmed GCTB (n=81; age 15–75 years; median age 33 years) and chondroblastoma (n=18; age 12–34 years; median age 14 years). In all, 18 imaging signs were analyzed.

Results: Patients with chondroblastoma were relatively younger than those with GCTB. On imaging, lesion length was significantly (P<0.00001) smaller in chondroblastoma [range, 15.80–78.30 mm; mean ± standard deviation (SD) 34.15±18.24 mm; 95% confidence interval (CI): 24.05–44.25 mm] than in GCTB [range, 30.10–117.50 mm; mean ± SD 59.73±15.28 mm; 95% CI: 56.24–63.22 mm]. Significantly more (P<0.05) chondroblastoma lesions had calcification (76.5% *vs.* 1.3%), lobulation (77.8% *vs.* 32.1%), and swelling range >15 mm (84.6% *vs.* 41.1%) than did GCTB lesions, whereas significantly more (P<0.05) GCTB lesions were greater than half the host bone diameter (74.1% *vs.* 16.7%) and had a lesion long axis that was consistent with that of the host bone (98.8% *vs.* 27.8%). There were no significant differences (P>0.05) between the 2 tumors in the remaining 11 imaging signs.

Conclusions: A narrow zone of transition, intratumor calcification, lobulation, tumor transverse diameter greater than the bone diameter, maximum lesion length, consistency between the tumor and bone long axes, and edema range around the lesion >15 mm are parameters that can be used to differentiate GCTB from chondroblastoma around the knee.

Keywords: Bone; chondroblastoma; giant cell tumor; imaging; knee

Submitted Jun 16, 2022. Accepted for publication Nov 30, 2022. Published online Jan 02, 2023.
doi: 10.21037/qims-22-616
View this article at: https://dx.doi.org/10.21037/qims-22-616

Introduction

Giant cell tumor of the bone (GCTB) was firstly described in 1818 (1) and is a relatively uncommon, aggressive, primary bone tumor that has a high risk of local recurrence following surgery. GCTB accounts for 4–5% of all primary bone tumors and 13–20% of all benign bone tumors (2,3). It occurs mostly in skeletally mature people, with a peak prevalence in the third and fourth decades of life at bones around the knee, followed by the distal radius and sacrum (2,4-6). Typical imaging features of GCTB include a purely lytic lesion with geographic bone destruction, an eccentric location, a well-defined but nonsclerotic margin, and extension to the subchondral bone (2,7). Nonaggressive GCTB exhibits prominent trabeculation with no soft tissue mass or cortical invasion; in contrast, aggressive lesions lack trabeculation and have cortical destruction or expansion associated with a soft tissue mass (2,4,7).

GCTBs have many common features on imaging with chondroblastoma and may present a challenge in terms of a correct diagnosis. Chondroblastoma is a rare primary benign osseous tumor that accounts for approximately 1% of all bone neoplasms, affecting mostly children and young adults in the second and third decades of life (8,9). Typically, chondroblastoma is located in the medullary cavity of the long bone epiphyses and apophyses, and is rarely found in the cortex or long bone metaphysis (8,9). The imaging features of these 2 tumors reported in previous studies (7,10-17) are summarized in *Table 1*. Because these 2 lesions have some common imaging presentations, their correct diagnosis and differentiation is of crucial clinical significance. Immunohistochemistry and gene detection are advanced methods for the diagnosis and differential diagnosis of different types of bone tumors. Schaefer *et al.* (18) suggested that the histones H3G34W and H3K36M are highly specific for GCTB and chondroblastoma, respectively, and are useful for the differentiation of these 2 tumors in limited biopsies. Venneker *et al.* (19) suggested that mutation-driven epigenetic alterations cause a highly altered transcriptome, resulting in changes that can be used to differentiate different diseases. Specific driver mutations have been discovered in chondroblastoma, GCTB, and central cartilaginous tumors that have the common ability to cause genome-wide epigenetic changes (20,21). In GCTB and chondroblastoma, the neoplastic mononuclear cells often harbor specific point mutations in genes encoding the histones H3F3A and H3F3B (19). The identification of these mutations has resulted in the development of new tools to differentiate chondroblastoma from GCTB, and these mutations induce several local and global changes in histone modification markers. However, imaging examinations are still the primary methods for the diagnosis and differential diagnosis of bone tumors, especially when immunohistochemistry and gene detection are not available.

GCTB and chondroblastoma around the knee joint, especially in the proximal tibia and distal femur, have many common imaging signs. Moreover, the ages at onset of these disease overlap, which makes differential diagnosis very difficult. Both tumors are benign and have aggressive growth potential; however, compared with chondroblastoma, GCTB is more invasive, with the edge sclerosis being less common on imaging than that of chondroblastoma. GCTB is more likely to recur after surgical curettage, with a worse prognosis (22). Chondroblastoma is usually less invasive and has a much lower recurrence rate than does GCTB (23,24). Therefore, differentiating between these 2 tumors will be helpful in guiding clinicians to choose suitable treatment methods.

The aim of this study was to investigate the clinical and imaging features of GCTB and chondroblastoma around the knee and to explore differences in imaging signs so as to provide important information for proper diagnosis and differentiation between these 2 tumors. We present the following article in accordance with the STROBE reporting checklist (available at https://qims.amegroups.com/article/view/10.21037/qims-22-616/rc).

Methods

This was a retrospective cross-sectional cohort study without follow-up. The study was conducted in accordance with the Declaration of Helsinki (as revised in 2013) and was approved by the Ethics Committee of the Third Hospital of Hebei Medical University. All patients or their legal guardians provided written informed consent. All methods were performed in accordance with the relevant guidelines and regulations.

Between January 2010 and December 2019, all patients diagnosed pathologically (by a senior pathologist with >10 years' experience) with GCTB and chondroblastoma at the distal femur and proximal tibia were enrolled. To be eligible for inclusion, patients had to have been diagnosed with GCTB and chondroblastoma around the knee joint, treated with surgery, and undergone pathological examination in the Third Hospital of Hebei Medical

Table 1 Imaging presentations of giant cell tumors of bone and chondroblastoma around the knee

Author (reference)	Year	No. patients	No. females/ males	Mean/median age (years)	Imaging presentations
He *et al.* (10)	2017	56	28/28	34/29	Fluid-fluid level in 23.2%, soap bubble sign in 28.6%, expansibility in 51.8%, osteosclerosis in 60.7%, adjacent soft tissue invasion in 66.1%, cystic change in 67.9%, cortical bone involvement in 83.9%
Liu *et al.* (15)	2016	3	3/0	22/20	17 lesions detected: 4 around the knee joint, 3 in the greater trochanter and head of the femur, 5 in the small bones of the feet, and 2 in flat bones
					Sclerotic margins or patchy sclerosis in 12 lesions, cortical discontinuity in 8, and soft tissue masses in 5
Herman *et al.* (11)	1987	3	3/0	NA/24	Pathological fractures, osteolysis, and soft tissue invasion
Levine *et al.* (7)	1984	15	9/6	29/27	Eccentricity in 93.3%, trabeculated pattern in 33.3%, marginal sclerosis in 20.0%, bone expansion in 46.7%, complete cortical penetration in 100%, subarticular cortical penetration in 46.7%, pathological fractures in 33.3%, periosteal reaction in 53.3%, and soft tissue mass in 33.3%
Liu *et al.* (16)	2019	36	12/24	17/16	Proximal tibia in 20, distal femur in 14, and patella in 2
					Physis was open in 10 patients, closing in 17, and closed in 9
					Invasion of the epiphysis plate in 7 patients; invasion of the articular cartilage in 8 patients
					Imaging signs included osteolytic lesions, a narrow zone of transition, no obvious sclerosis, scattered calcification, and lesions not crossing the articular cartilage and epiphyseal line
Lehner al. (14)	2011	24	8/16	17.4/NA	Distal femur in 6, proximal tibia in 6, proximal humerus in 8, and proximal femur in 4
					3 inactive lesions, 13 active lesions, and 8 aggressive lesions
John *et al.* (12)	2020	39	10/29	NA/25	An osteolytic lesion with a narrow zone of transition in 24 cases, a peripheral rim of sclerosis in 21, osseous expansion in 9, and a calcified matrix in 5
Xu *et al.* (17)	2015	199	54/145	NA/18	Intralesional mineralization in 83 (44.6%) patients, cortical destruction in 36 (19.4%) patients, and invasion of the physis in 39 (21.0%) patients
Jundt *et al.* (13)	2018	143	37/106	NA	Eccentric osteolysis, rosette-like outline, sclerotic margin, and punctate calcification in the osteolytic center

NA, not available.

University, with GCTB and chondroblastoma confirmed pathologically. Patients who had the disease located beyond the distal femur and proximal tibia and those with postoperative recurrence were excluded.

Clinical and imaging data [i.e., plain radiography, computed tomography (CT), and magnetic resonance imaging (MRI)] were assessed by 2 senior radiologists (ZW Zhong and L Cao) with >10 years' clinical experience (*Table 2*). If there was disagreement, data were assessed by a third researcher to reach an agreement. The following data were evaluated: age, sex, discontinuation in the cortex, pathologic fractures, well-defined margin, sclerotic margin, calcification inside the lesion, eccentric location, lobulation, lesion diameter and major axis compared with the long bone diameter, soft tissue masses, periosteal reaction, fluid-fluid level, bone septa, minimum distance from the lesion edge to the articular surface of the knee, maximum lesion diameter, edema around the lesion >15 mm, bone ridge, and

Table 2 Indices of giant cell tumor of the bone and chondroblastoma

Index	GCTB	CH	P value
No. of patients	81	18	N/A
No. of males/females	34/47	16/2	
Age (years)			
Median (IQR)	33 (9.5)	14 (8.5)	
25th–75th percentile	27–36	13–21	
Range	15–75	12–34	
Imaging (n)			
DR	58	14	
CT	67	14	
MRI	56	13	
DR + CT	78	17	
CT + MRI	76	15	
Distance between tumor and joint surface (mm)			0.11
Mean ± SD	2.23±3.47	7.35±10.44	
95% CI	1.44–3.02	1.57–13.13	
Range	0–16.70	0–30.50	
Maximum length (mm)			<0.01
Mean ± SD	59.73±15.28	34.15±18.24	
95% CI	56.23–63.22	24.05–44.25	
Range	30.10–117.50	15.80–78.30	
Maximum length distribution (n)			N/A
0 mm < length ≤20 mm	0	3	
20 mm < length ≤40 mm	6	6	
40 mm < length ≤60 mm	35	3	
60 mm < length ≤80 mm	29	3	
80 mm < length ≤100 mm	5	0	
Length >100 mm	1	0	
Discontinued bone cortex	67 (82.7)	16 (88.9)	0.73
Pathological fracture	19 (23.5)	2 (11.1)	0.35
Narrow zone of transition	14 (24.1)	12 (85.7)	<0.01
Sclerotic margin	53 (67.9)	14 (82.4)	0.24
Breaking physeal plate	4 (4.9)	5 (27.8)	N/A
Intratumor calcification	1 (1.3)	13 (76.5)	<0.01
Eccentric	72 (88.9)	16 (88.9)	1.00

Table 2 (*continued*)

Table 2 (*continued*)

Index	GCTB	CH	P value
Lobulated	26 (32.1)	14 (77.8)	<0.01
Tumor transverse diameter >½ of host bone	60 (74.1)	3 (16.7)	<0.01
Soft tissue mass	12 (14.8)	0 (0)	0.12
Axis along the long bone	80 (98.8)	5 (27.8)	<0.01
Periosteal reaction	13 (16.0)	3 (16.7)	1.00
Fluid-fluid level	10 (17.9)	2 (15.4)	1.00
Bone septum	1 (1.5)	2 (14.3)	0.07
Bone ridge	63 (82.9)	13 (86.7)	1.00
Swelling range >15 mm	23 (41.1)	11 (84.6)	0.01

Unless indicated otherwise, data are given n (%). CH, chondroblastoma; CI, confidence interval; CT, computed tomography; DR, digital radiography; GCTB, giant cell tumor of the bone; IQR, interquartile range; MRI, magnetic resonance imaging; N/A, not applicable.

penetration of the epiphyseal plate (*Table 2*).

The equipment used in this study was a 500-mA Siemens DR system, Siemens 16- and 64-slice CT scanners, and a Siemens Symphony 1.5 T magnetic resonance (MR) scanner (Siemens Healthineers, Erlangen, Germany). The parameters for the CT scanners were as follows: collimator, 0.6 mm; pitch, 1; tube voltage, 120 kV; automatic milliampere technique; reconstruction thickness, 1 mm; and thickness of multiplanar reformations, 3 mm. The major imaging sequences for MRI scanning were spin echo (SE) T_1-weighted image (T1WI) [repetition time (TR), 500 ms; time to echo (TE) 15 ms; matrix, 512×512; field of view (FOV), 160 mm; thickness, 4 mm; and interval, 0.8 mm], turbo spin echo (TSE) T_2-weighted image (T2WI) (TR, 2,500 ms; TE, 90 ms; matrix, 512×512; FOV, 160 mm; thickness, 4 mm; and interval, 0.8 mm), and short TI inversion recovery (STIR) [TR, 3,700 ms; inversion time (TI), 160 ms; flip angle, 15°; matrix, 256×256; FOV, 160 mm; thickness, 3.5 mm; and interval, 1.05 mm], including cross-sectional, coronal and sagittal planes. The software used for measurement was that provided with the scanning system.

Discontinued bone cortex was defined as discontinuation of the bone cortex, with sclerotic rims indicating the boundary of the lesion that had a greater density than surrounding areas. Bone septa or separations were located inside the lesion on CT planes, and bone crests or ridges were referred to as bone protuberances inside the lesion on CT or MRI images. The minimum distance from the lesion edge to the joint bone surface was measured in the coronal or sagittal plane on either CT or MRI images (*Table 2*). The maximum length of the lesion was measured in the sagittal plane on CT or MRI images, and lesion length was divided into 6 groups: 0–20, 21–40, 41–60, 61–80, 81–100, and >100 mm (*Table 2*). The maximal MRI plane which displayed the best swelling of the lesion was chosen for relevant measurement, and patients with pathological fractures or bad imaging quality that could affect precise measurement were excluded.

Statistical analysis

Statistical analyses were performed using SPSS 19.0 (IBM Corp., Armonk, NY, USA). There were no missing data in this cross-sectional study. Normally distributed continuous variables are presented as the mean ± standard deviation (SD), whereas continuous variables that were not normally distributed are presented as the median and interquartile range (IQR). Categorical variables are presented as counts and percentages. The significance of differences in the distance from the lesion edge to the knee joint surface was tested using the rank-sum test, whereas the significance of differences in all other indices was tested using the chi-squared test. The maximum length of the sclerotic rims of the 2 benign tumors was compared with the lesion perimeter and analyzed using receiver operator characteristic (ROC) curves for a proper proportion for better diagnosis. Significance was set at a two-tailed P value <0.05.

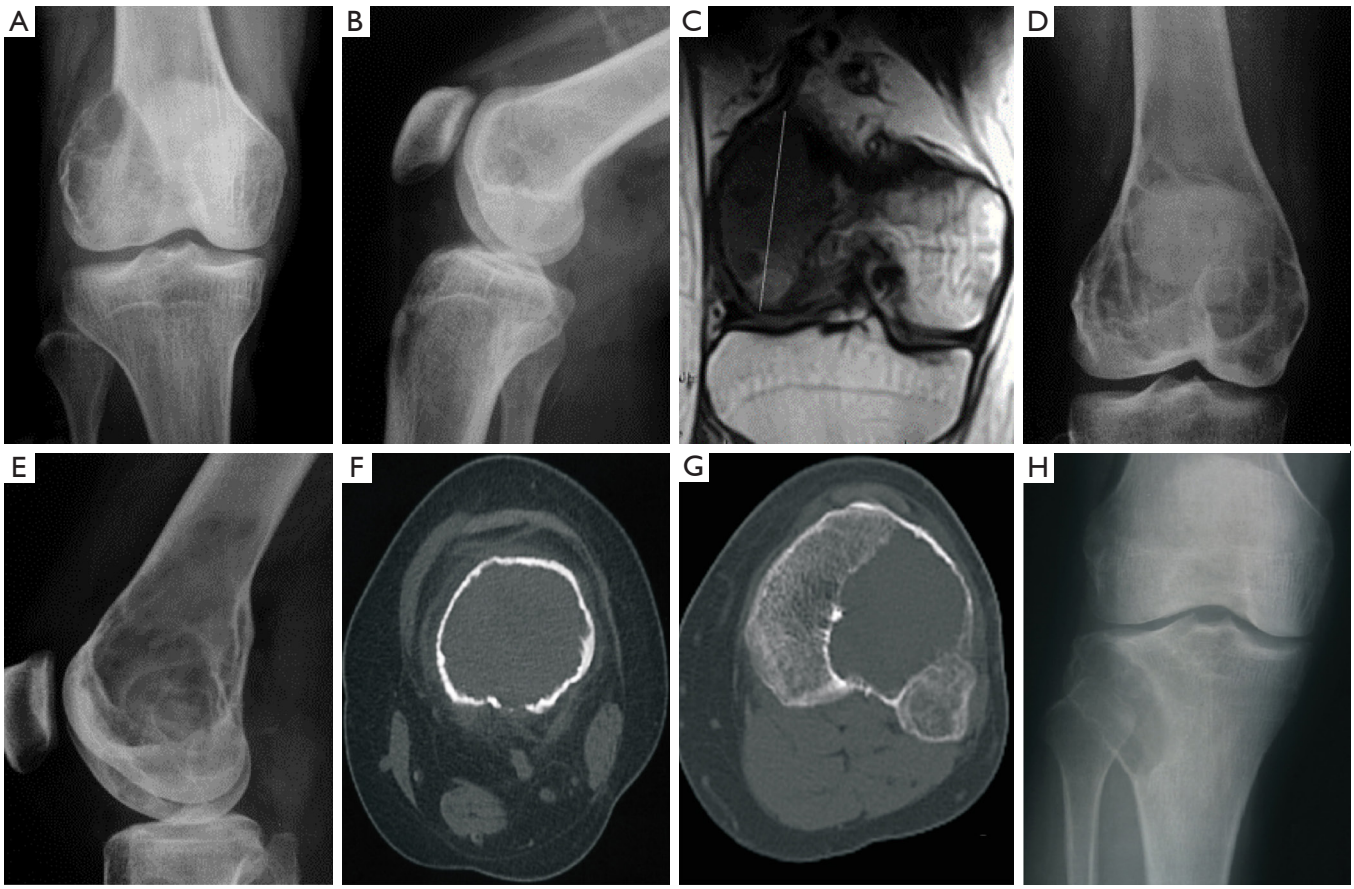

Figure 1 Giant cell tumors of the bone. (A-E) Images are from 1 patient. (A,B) Plain radiography showed an eccentric, expansile, lytic lesion on the lateral condyle of the right femur with a narrow zone of transition, extending down to the joint surface with a thin bony cortex and fine ridges. (C) Magnetic resonance imaging T1-weighted image on the coronal plane demonstrated the lesion to have a nonuniform long T1 signal with a limited range of disease and a clear boundary. (D,E) Plain radiography revealed a big, expansile, lytic lesion in the distal end of the right femur, extending downward to the joint surface and upward to the bone diaphysis with coarse bone ridges inside. (F-H) Images from another patient. (F) CT showed expansile destruction in the distal end of the left tibia with uniform density and disrupted cortical bone but no apparent sclerotic margins. No soft tissue mass was present. (G) CT revealed an expansile eccentric destruction at the proximal end of the left tibia bone with uniform intratumor density, a partial sclerotic margin, and no soft tissue mass. (H) Plain radiography demonstrated expansile eccentric destruction at the lateral condyle of the right tibia with uniform intratumor density and a partial sclerotic margin. CT, computed tomography.

Results

In all, 81 patients (34 males, 47 females) with GCTB (*Figures 1*,*2*) and 18 patients (16 males, 2 females) with chondroblastoma (*Figure 3*) around the knee were identified and enrolled in this study (*Figure 4*). The median age of the 81 patients with GCTB was 33 years (IQR, 9.5 years; 25th–75th percentile, 27–36 years; range, 15–75 years). The median age of the 18 patients with chondroblastoma was 14 years (IQR, 8.5 years; 25th–75th percentile, 13–21 years; range, 12–34 years). Patients with chondroblastoma were relatively younger than those with GCTB (*Figure 5A*). The disease prevalence of the 2 tumors overlapped for ages 21–30 years, which included 31 (38.3%) patients with GCTB and 4 (22.2%) patients with chondroblastoma, accounting for 38.3% and 22.2% of cases in each group, respectively. In addition, 3 patients with GCTB were 10–20 years of age (the peak age range for chondroblastoma), and 1 patient with chondroblastoma was aged 34 years (falling within the peak age range of 31–40 years for GCTB).

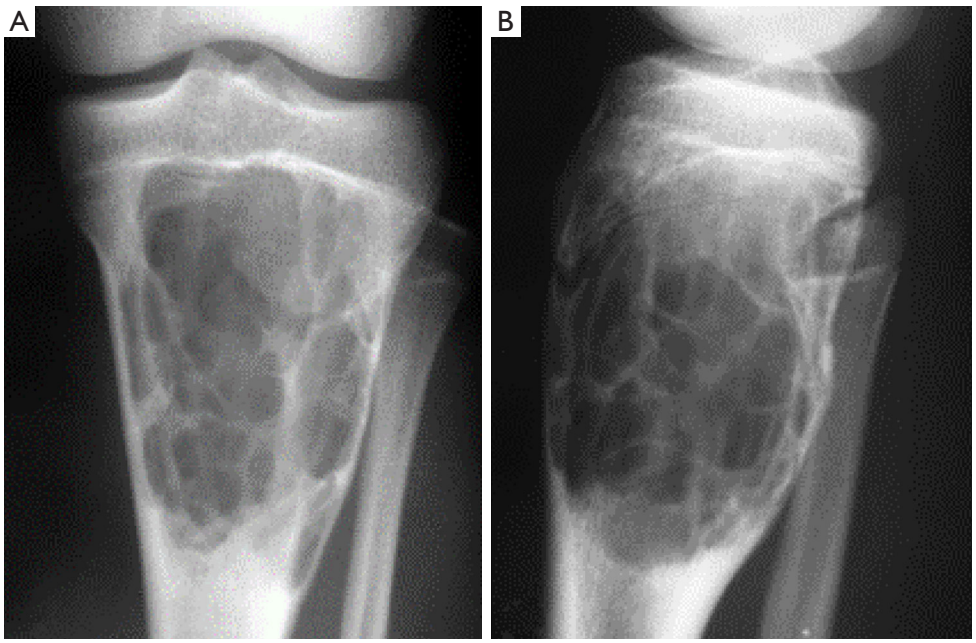

Figure 2 Giant cell tumor of the bone. Plain radiography of the anteroposterior (A) and lateral positions (B) showed an expansile lesion with multiple cysts at the metaphysis of the proximal tibia. Some coarse bony ridges were inside the lesion, and the lesion did not break the epiphysis.

Of the 81 patients with GCTB, 58 underwent plain radiography, 67 underwent CT, 56 underwent MRI, 78 underwent both plain radiography and CT, and 76 underwent both CT and MRI (*Table 2*). Of the 81 patients with GCTB, 50 had a lesion at the distal end of the femur (*Figure 1*), with the lesion being eccentric and lytic with fine or coarse bone ridges on plain radiography. On MRI, GCTB lesions presented as a nonuniform low T1WI signal with a limited range of disease and a clear boundary (*Figure 1C*). Another 31 GCTB lesions were located at the proximal end of the tibia (*Figures 2,3*), with the lesion being expansile and lytic on plain radiography, presenting with intratumor uniform density, a partial sclerotic margin, and coarse bone ridges. The lesion did not penetrate the epiphysis. On CT imaging (*Figure 2*), the lesion was lytic and had uniform density and a disrupted cortical bone, but there was no apparent sclerotic margin or soft tissue inside the lesion.

Of the 18 cases of chondroblastoma, 9 were at the distal end of the femur (*Figure 3*) and the other 9 were at the proximal end of the tibia (*Figure 3A,3B*). On CT imaging, the lesion showed lytic bone destruction at the distal end of the femur, with no bone septa or calcification inside the lesion. The boundary of the lesion was well-defined with sclerosis (*Figure 3*). Some lesions had nonuniform density inside the tumor, an apparent sclerotic margin, and an intratumor bony septum (*Figure 3*). On MRI, the lesions had a hyperintense T_2 signal with lobulated changes and bone ridges inside the lesion (*Figure 3*). Some lesions had nonuniform hypointense T_1 but hyperintense T_2 signals and had invaded the soft tissue on the lateral side (*Figure 3*).

In patients with GCTB, the mean distance from the lesion to the knee joint surface was 2.23±3.47 mm [range, 0–16.70 mm; 95% confidence interval (CI): 1.44–3.02 mm; *Table 2*]. In chondroblastoma, the mean from the lesion to the knee joint surface was 7.35±10.44 mm (range, 0–30.50 mm; 95% CI: 1.57–13.13 mm), which was not significantly different compared with GCTB lesions (P=0.11; *Table 2*).

For GCTB, the maximum length of the lesion was 21–40 mm in 6 patients, 41–60 mm in 35 patients, 61–80 mm in 29 patients, 81–100 mm in 5 patients, and >100 mm in only 1 patient, with a mean maximum length of 59.73±15.28 mm (range 30.10–117.50 mm; 95% CI: 56.23–63.22 mm; *Table 2*). In chondroblastoma, the maximum length of the lesion was 0–20 mm in 3 patients, 21–40 mm in 6 patients, 41–60 in 3 patients, and 61–80 mm in 3 patients, with a mean maximum length of 34.15±18.24 mm (range, 15.80–78.30 mm; 95% CI: 24.05–

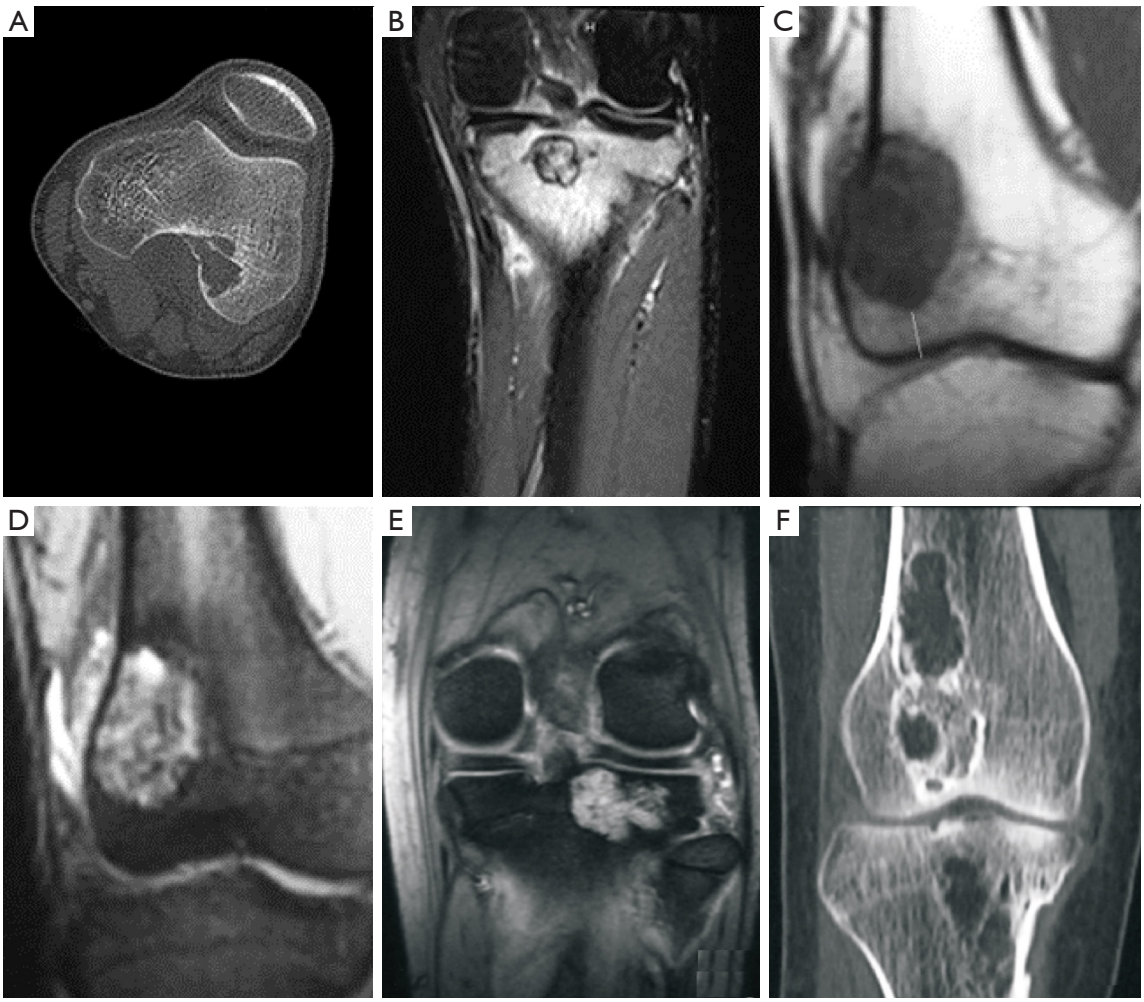

Figure 3 Chondroblastoma. (A-D) Images from 1 patient. (A) CT revealed lytic destruction at the distal end of the femur with a well-defined and sclerotic boundary but no bone septa or calcification. (B) An area with a long T2 signal was present at the proximal end of the left tibia, with lobulated changes and bone ridges. Adjacent bone marrow and soft tissue showed swelling signals. (C,D) Lytic destruction was revealed on MRI T1-weighted (C) and T2-weighted (D) images with non-uniform long T1 and long T2 signals and soft tissue being invaded on the lateral side. (E,F) Images from another patient. (E) MRI showed an irregular area with a long T2 signal with bone crests and lobulated changes at the proximal end of the tibia. (F) CT showed a recurrent chondroblastoma lesion at the distal end of the left femoral bone and proximal end of the tibia with nonuniform density, an apparent sclerotic margin, and an intratumoral bony septum. CT, computed tomography; MRI, magnetic resonance imaging.

44.25 mm); this was significantly smaller (P<0.001) than the mean maximum length of GCTB lesions (*Table 2*).

A narrow zone of transition was seen in 14 cases of GCTB and in 12 cases of chondroblastoma. In the GCTB group, 53 patients had sclerotic rims, including 47 with partial sclerotic rims and 42 with the maximum length of the sclerotic rim <25% of the lesion perimeter (*Table 2*). In the chondroblastoma group, 14 patients had sclerotic rims, including 8 with partial sclerotic rims, and the maximum length of the sclerotic rim accounted for 35% of the lesion perimeter. There was no significant difference in the presence of a sclerotic margin between the GCTB and chondroblastoma groups (P=0.24; *Table 2*), but the ratio of sclerotic edge length to lesion circumference was significantly smaller for GCTB than for chondroblastomas [15.0 (46.3) *vs.* 70.0 (60.0); P=0.007]. ROC curve analysis of the proportion of the lesion sclerotic rim to the lesion perimeter revealed no appropriate cutoff value to

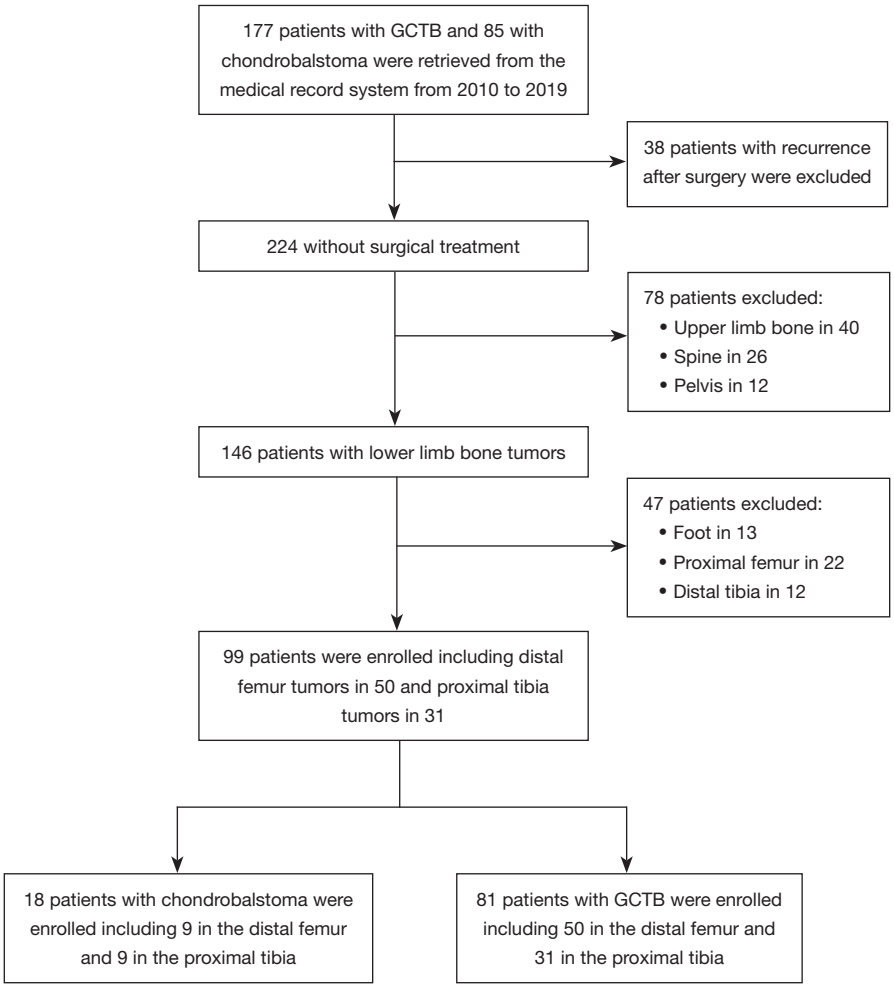

Figure 4 Flowchart showing the enrollment of patients with GCTB and patients with chondroblastoma at the knee. GCTB, giant cell tumors of the bone.

differentiate these 2 tumors (*Figure 5*). Two patients with chondroblastomas had bone septa within the lesion (*Table 2*).

Analysis of 16 imaging parameters between the GCTB and chondroblastoma groups (*Table 3*) revealed significant differences (P<0.05) in the narrow zone of transition (24.1% *vs.* 85.7%, respectively), intratumor calcification (1.3% *vs.* 76.5%, respectively), lobulation (32.1% *vs.* 77.8%, respectively), tumor transverse diameter greater than half the long bone diameter (74.1% *vs.* 16.7%, respectively), consistency between the tumor and bone long axes (98.8% *vs.* 27.8%, respectively), and swelling range >15 mm (41.1% *vs.* 84.6%, respectively) that could be used to differentiate GCTB from chondroblastoma (*Table 2*).

Discussion

In this study, of the imaging presentations evaluated, a narrow zone of transition, intratumor calcification, lobulation, tumor transverse diameter greater than half the diameter of the long bone, maximum length, consistency between the tumor and bone long axes, and edema around the lesion >15 mm were statistically significant parameters to differentiate GCTB from chondroblastoma around the knee (*Table 3*).

The knee is a predilection site for both GCTB and chondroblastoma, and both tumors may have imaging characteristics of lytic bone destruction, expansile growth, eccentric location, and sclerotic margins, with clinical

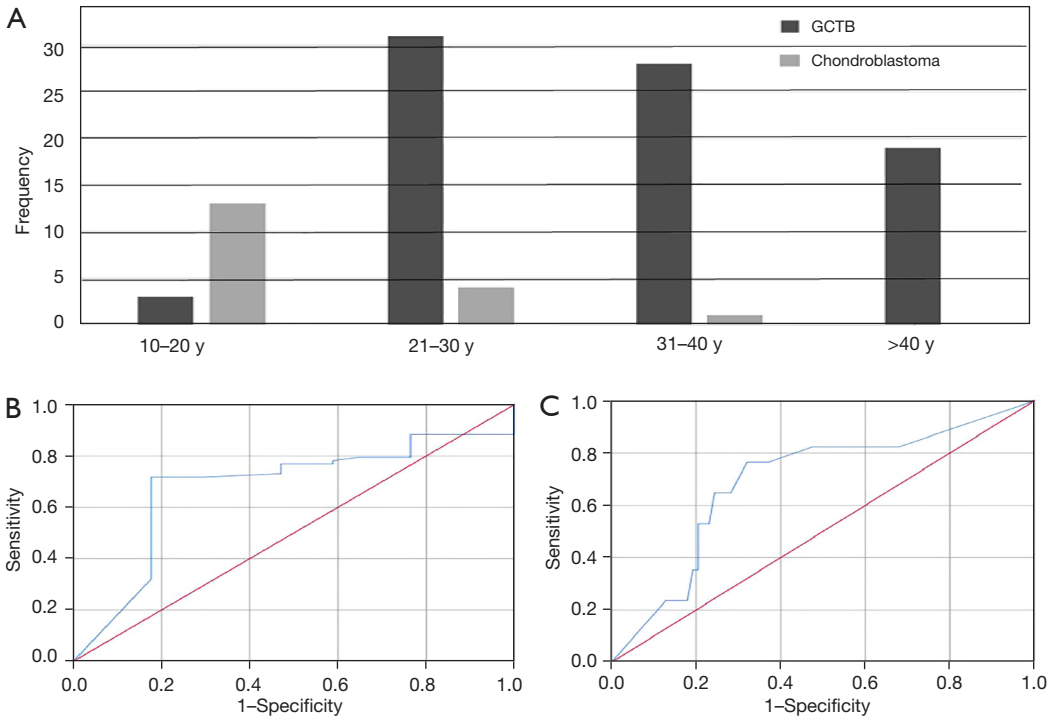

Figure 5 Age distribution and ROC curve analysis of the lesion sclerotic rim to the perimeter. (A) Age distribution of patients with GCTB and chondroblastoma around the knee. (B,C) ROC curve analysis of the proportion of the lesion sclerotic rim to the lesion perimeter for GCTB (B) and chondroblastoma (C). The AUC for GCTB and chondroblastoma was 0.68 (P=0.02) and 0.69 (P=0.01), respectively; in both cases, the AUC was <0.7, indicating a low accuracy of diagnosis. AUC, area under the curve; GCTB, giant cell tumors of the bone; ROC, receiver operator characteristic.

Table 3 Clinical significance of imaging signs

Variable	Narrow zone of transition	Intratumor calcification	Lobulated	Tumor transverse diameter >½ of host bone	Axis along the long bone	Swelling range >15 mm
Tumor, n (%)						
GCTB	14 (24.1)	1 (1.3)	26 (32.1)	60 (74.1)	80 (98.8)	23 (41.1)
CH	12 (85.7)	13 (76.5)	14 (77.8)	3 (16.7)	5 (27.8)	11 (84.6)
Differentiation	GCTB is more invasive than CH	Calcification is a feature of chondroid tumors; CH has a higher rate of calcification	CH is usually characteristically lobular which is related to its slow growth	CH is usually small, with the transverse diameter <½ the diameter of the long bone; GCTB is expansive with the diameter >½ the bone diameter	GCTB tends to grow along the long axis of the long bone; CH tends to grow laterally, with the long axis of the lesion not consistent with that of the bone	One MRI feature of CH is soft tissue edema

Unless indicated otherwise, data are given as n (%). CH, chondroblastoma; GCTB, giant cell tumor of the bone; MRI, magnetic resonance imaging.

symptoms of local pain and swelling (*Figures 1*,*2*). Age may have certain value in differentiating GCTB from chondroblastoma, with chondroblastoma occurring in patients aged <20 years and GCTB in patients aged >30 years; however, it should be noted that these tumors have an age overlap between 20 and 30 years. In the present case series, 38.8% of GCTB patients and 22.2% of chondroblastoma patients were within the overlapping age range of 21–30 years.

The ability of GCTB to invade surrounding tissues is greater than that of chondroblastoma, which is why GCTB had a wide zone of transition. Intratumor mottled or stippled calcification occurred in 70% of all cases of chondroblastoma and presenting like grains of sand, primarily caused by calcification of the basophilic matrix around chondrocytes in the cartilage tumors. The incidence of calcification was high in this series, probably because CT is sensitive in detecting small calcification, thus improving the detection rate of calcification. However, internal calcification has been rarely reported for GCTB.

Although the distance from the lesion edge to the articular surface was greater for chondroblastoma than for GCTB lesions, the difference did not reach statistical significance (P>0.05). In addition to GCTB, there are other tumors, such as telangiectatic osteosarcoma, giant cell rich osteosarcoma, and clear cell chondrosarcoma, that may be primarily located at or involve bone ends and need to be differentiated from GCTB. If a tumor lesion is near the articular cortex, GCTB should be considered because these lesions usually occur at the bone end, whereas chondroblastoma lesions mostly occur at or near the epiphyseal plate. Using equations fitted to regression models, Futamura *et al.* found that GCTB arising in long bones in 71 patients probably originated from the metaphyseal region (25). In addition, among these 71 patients, the distance between the articular surface and the GCTB tumor border was short, even in cases of small tumors (25). This is consistent with other studies that report that approximately 84–99% of GCTB lesions extended to within 1 cm of subarticular bone (26,27).

In our study, intratumor calcification, lobulation, tumor transverse diameter greater than half the diameter of the long bone, maximum length, consistency between the tumor and bone long axes, and edema around the lesion >15 mm were statistically significant parameters to differentiate GCTB from chondroblastoma around the knee. The intratumor calcification rate of chondroblastoma was 76.5%, with small dots or sand-like calcification, which is caused primarily by calcification of the basophil matrix around chondrocytes in chondroid tumors (2). Intratumor calcification is rarely seen in GCTB. Tumor lobulation is usually caused by different growth rates in various directions or the blocking of tumor growth by surrounding structures, resulting in a tumor contour with multiple protrusions. Chondroblastoma often presents as a shallow lobulated or shallow wavy lesion, which has no obvious relationship with the size of the tumor. Both GCTB and chondroblastoma can grow expansively; however, because chondroblastoma lesions are usually small, most are smaller than half the diameter of the long bone. GCTBs are usually big with expansive growth, and the lesion diameter is mostly greater than the diameter of the long bone. Because the expansive growth of GCTB is usually greater than that of chondroblastoma, especially along the long axis of the bone, the long axis of the GCTB tumor is usually consistent with that of the bone. However, chondroblastoma tends to grow laterally, with only a few tumors having the long axes consistent with the tumor-bearing bone. GCTB is usually found late because it has no clinical symptoms, resulting in large lesion volume, whereas chondroblastoma is often associated with local pain, most of which is chronic and accompanied by swelling of the surrounding soft tissue. Thus, chondroblastoma is found earlier at a small size. In this study, the maximum length of the lesion was 40–80 mm for GCTB and 20–40 mm for chondroblastoma. Therefore, chondroblastoma is more likely when the maximum length of the tumor is <40 mm with no knee pain caused by obvious exogenous factors or sports system injury (e.g., trauma, fracture, meniscus and ligament injury), whereas GCTB is more likely when local symptoms around the knee joint are mild and the maximum length of the tumor is >40 mm. Histopathological examination of chondroblastoma typically shows fluid exudation and inflammatory cell infiltration in the area of bone marrow edema (28), resulting in edema around the lesion >15 mm. Clinically, patients often present with local pain and peritumoral bone marrow edema, accompanied (or not) by surrounding soft tissue edema. Although the volume of GCTB is usually large at diagnosis, the incidence and range of the edema are small.

Some imaging presentations did not contribute to differentiation. A sclerotic margin is a reactive change of the body and reflects the growth rate of a lesion, which can be used for determining the invasiveness of a lesion. There was no significant difference in the frequency of the presence of sclerotic edges between the GCTB and chondroblastoma

groups in this study, but the ratio of sclerotic edge length to lesion circumference was significantly smaller (P=0.007) for GCTB than it was for chondroblastoma. This is consistent with other studies, which reported that typical chondroblastoma had mottled calcification and a peripheral sclerotic margin, whereas GCTB lacked a complete sclerotic rim and visible internal calcification (1,8). This finding is helpful for the differentiation of GCTB and chondroblastoma, but ROC analysis of the length of the sclerotic margin revealed no appropriate cutoff value to differentiate these 2 tumors.

Traditionally, GCTBs are considered to have a discontinued bone cortex in most cases. However, in this study, more cases of chondroblastoma had cortical disruption, although there was no significant difference (P>0.05) between the 2 groups. This is probably related to the expansile growth with more osteoclast activity inside the chondroblastoma lesion. When the lesion breaks the cortex with a soft tissue mass appear, the nature of the invasiveness is suggested by the biological behavior (29). Eccentric growth is part of the development process of tumors and is a characteristic of GCTB; however, in the present study, a similar percentage of both types of lesions had eccentric growth.

Chondroblastoma may cause periostitis and subsequent periosteal proliferation, which may be useful for the differentiation of the 2 tumors. In this study, all patients with GCTB with a periosteal reaction had a pathological fracture, and the periosteal reaction might have been related to bone fracture. Bone septum with the appearance of soap bubbles is a typical radiological feature of GCTB; in this study, this appearance was evident in only 2 patients with recurrent chondroblastoma and was probably caused by postoperative repair and recurrence. When chondroblastoma is concurrent with a secondary aneurysmal bone cyst, bone septa with a beehive appearance may be present (30).

This study has some limitations, including a small cohort of patients, an exclusive enrollment of Chinese patients, and a single-center, retrospective design. Future prospective studies are needed in multiple centers to overcome these limitations. Although the present study was a retrospective descriptive study, all the GCTBs and chondroblastomas had been confirmed pathologically. All indices evaluated of the tumors were measured twice by 2 researchers, which provides confidence in the accuracy of the measurement results and maintains certain external authenticity.

Conclusions

Imaging signs provide some valuable information for the differentiation of GCTB from chondroblastoma. On medical imaging, a narrow zone of transition, intratumor calcification, lobulation, a tumor transverse diameter greater than half the diameter of the long bone, maximum length, consistency between the long axis of the tumor and bone, and edema around the lesion >15 mm are statistically significant parameters to differentiate GCTB from chondroblastoma around the knee. A large tumor with small edema indicates GCTB, whereas a small tumor with large edema supports the diagnosis of chondroblastoma.

Acknowledgments

Funding: None.

Footnote

Reporting Checklist: The authors have completed the STROBE reporting checklist. Available at https://qims.amegroups.com/article/view/10.21037/qims-22-616/rc

Conflicts of Interest: All authors have completed the ICMJE uniform disclosure form (available at https://qims.amegroups.com/article/view/10.21037/qims-22-616/coif). The authors have no conflicts of interest to declare.

Ethical Statement: The authors are accountable for all aspects of the work in ensuring that questions related to the accuracy or integrity of any part of the work are appropriately investigated and resolved. The study was conducted in accordance with the Declaration of Helsinki (as revised in 2013). This study was approved by the Ethics Committee of the Third Hospital of Hebei Medical University, and all patients or their legal guardians provided written informed consent.

References

1. Sobti A, Agrawal P, Agarwala S, Agarwal M. Giant Cell Tumor of Bone - An Overview. Arch Bone Jt Surg 2016;4:2-9.
2. Chakarun CJ, Forrester DM, Gottsegen CJ, Patel DB, White EA, Matcuk GR Jr. Giant cell tumor of bone: review, mimics, and new developments in treatment. Radiographics 2013;33:197-211.
3. Niu X, Zhang Q, Hao L, Ding Y, Li Y, Xu H, Liu W. Giant cell tumor of the extremity: retrospective analysis of 621 Chinese patients from one institution. J Bone Joint Surg Am 2012;94:461-7.
4. Mavrogenis AF, Igoumenou VG, Megaloikonomos PD, Panagopoulos GN, Papagelopoulos PJ, Soucacos PN. Giant cell tumor of bone revisited. SICOT J 2017;3:54.
5. Randall RL. Giant cell tumor of the sacrum. Neurosurg Focus 2003;15:E13.
6. Ruggieri P, Mavrogenis AF, Ussia G, Angelini A, Papagelopoulos PJ, Mercuri M. Recurrence after and complications associated with adjuvant treatments for sacral giant cell tumor. Clin Orthop Relat Res 2010;468:2954-61.
7. Levine E, De Smet AA, Neff JR. Role of radiologic imaging in management planning of giant cell tumor of bone. Skeletal Radiol 1984;12:79-89.
8. Wang F, Li J, Yu D, Wang Q. Chondroblastoma of the distal femoral metaphysis: A case report with emphasis on imaging findings and differential diagnosis. Medicine (Baltimore) 2018;97:e0336.
9. Zheng J, Niu N, Shi J, Zhang X, Zhu X, Wang J, Liu C. Chondroblastoma of the patella with secondary aneurysmal bone cyst, an easily misdiagnosed bone tumor:a case report with literature review. BMC Musculoskelet Disord 2021;22:381.
10. He Y, Wang J, Zhang J, Yuan F, Ding X. A prospective study on predicting local recurrence of giant cell tumour of bone by evaluating preoperative imaging features of the tumour around the knee joint. Radiol Med 2017;122:546-55.
11. Herman SD, Mesgarzadeh M, Bonakdarpour A, Dalinka MK. The role of magnetic resonance imaging in giant cell tumor of bone. Skeletal Radiol 1987;16:635-43.
12. John I, Inwards CY, Wenger DE, Williams DD, Fritchie KJ. Chondroblastomas presenting in adulthood: a study of 39 patients with emphasis on histological features and skeletal distribution. Histopathology 2020;76:308-17.
13. Jundt G, Baumhoer D. Chondroblastoma. Pathologe 2018;39:132-8.
14. Lehner B, Witte D, Weiss S. Clinical and radiological long-term results after operative treatment of chondroblastoma. Arch Orthop Trauma Surg 2011;131:45-52.
15. Liu C, Tang Y, Li M, Jiao Q, Zhang H, Yang Q, Yao W. Clinical characteristics and prognoses of six patients with multicentric giant cell tumor of the bone. Oncotarget 2016;7:83795-805.
16. Liu Q, He H, Yuan Y, Zeng H, Long F, Tian J, Luo W. Have the difficulties and complications of surgical treatment for chondroblastoma of the adjoining knee joint been overestimated? J Bone Oncol 2019;17:100240.
17. Xu H, Nugent D, Monforte HL, Binitie OT, Ding Y, Letson GD, Cheong D, Niu X. Chondroblastoma of bone in the extremities: a multicenter retrospective study. J Bone Joint Surg Am 2015;97:925-31.
18. Schaefer IM, Fletcher JA, Nielsen GP, Shih AR, Ferrone ML, Hornick JL, Qian X. Immunohistochemistry for histone H3G34W and H3K36M is highly specific for giant cell tumor of bone and chondroblastoma, respectively, in FNA and core needle biopsy. Cancer Cytopathol 2018;126:552-66.
19. Venneker S, Szuhai K, Hogendoorn PCW, Bovée JVMG. Mutation-driven epigenetic alterations as a defining hallmark of central cartilaginous tumours, giant cell tumour of bone and chondroblastoma. Virchows Arch 2020;476:135-46.
20. Cleven AH, Höcker S, Briaire-de Bruijn I, Szuhai K, Cleton-Jansen AM, Bovée JV. Mutation Analysis of H3F3A and H3F3B as a Diagnostic Tool for Giant Cell Tumor of Bone and Chondroblastoma. Am J Surg Pathol 2015;39:1576-83.
21. Gong L, Bui MM, Zhang W, Sun X, Zhang M, Yi D. H3F3A G34 mutation DNA sequencing and G34W immunohistochemistry analysis in 366 cases of giant cell tumors of bone and other bone tumors. Histol Histopathol 2021;36:61-8.
22. Suzuki T, Kaneuchi Y, Hakozaki M, Yamada H, Yamada S, Konno S. Visualization of hidden soft-tissue recurrence of giant cell tumor of bone enabled by preoperative denosumab treatment: a case description. Quant Imaging Med Surg 2021;11:3893-7.
23. Huang C, Lü XM, Fu G, Yang Z. Chondroblastoma in the Children Treated with Intralesional Curettage and Bone Grafting: Outcomes and Risk Factors for Local

Recurrence. Orthop Surg 2021;13:2102-10.
24. Tsukamoto S, Mavrogenis AF, Hindiskere S, Honoki K, Kido A, Fujii H, Masunaga T, Tanaka Y, Chinder PS, Donati DM, Errani C. Outcome of Reoperation for Local Recurrence Following En Bloc Resection for Bone Giant Cell Tumor of the Extremity. Curr Oncol 2022;29:6383-99.
25. Futamura N, Urakawa H, Tsukushi S, Arai E, Kozawa E, Ishiguro N, Nishida Y. Giant cell tumor of bone arising in long bones possibly originates from the metaphyseal region. Oncol Lett 2016;11:2629-34.
26. Hudson TM, Schiebler M, Springfield DS, Enneking WF, Hawkins IF Jr, Spanier SS. Radiology of giant cell tumors of bone: computed tomography, arthro-tomography, and scintigraphy. Skeletal Radiol 1984;11:85-95.
27. Murphey MD, Nomikos GC, Flemming DJ, Gannon FH, Temple HT, Kransdorf MJ. From the archives of AFIP. Imaging of giant cell tumor and giant cell reparative granuloma of bone: radiologic-pathologic correlation. Radiographics 2001;21:1283-309.
28. Martin JR, Auran RL, Duran MD, de Comas AM, Jacofsky DJ. Management of Primary Aggressive Tumors of the Knee. J Knee Surg 2022;35:585-96.
29. Raskin KA, Schwab JH, Mankin HJ, Springfield DS, Hornicek FJ. Giant cell tumor of bone. J Am Acad Orthop Surg 2013;21:118-26.
30. Gutierrez LB, Link TM, Horvai AE, Joseph GB, O'Donnell RJ, Motamedi D. Secondary aneurysmal bone cysts and associated primary lesions: imaging features of 49 cases. Clin Imaging 2020;62:23-32.

Cite this article as: Ma JL, Wu Y, Wen JX, Zhong ZW, Yu BH, Liu C, Cao L, Sun T, Han SM, Gao BL, Wu WJ. Images of giant cell tumor and chondroblastoma around the knee: retrospective analysis of 99 cases. Quant Imaging Med Surg 2023;13(2):787-800. doi: 10.21037/qims-22-616